Noise and Transfer Properties of Harmonically Synchronized Oscillators

REINHARD KNÖCHEL AND KLAUS SCHÜNEMANN, MEMBER, IEEE

Abstract—**A theoretical model of a harmonically synchronized oscillator is developed. Using this model output power, stability conditions, noise, and transfer properties of a harmonic frequency divider are calculated and discussed.**

I. Introduction

HARMONIC synchronization of a free-running oscillator is a powerful means for performing frequency division in the microwave region. A possible application of such a divider circuit lies in an indirect amplification system for FM signals, which consists of a frequency divider, a power amplifier in the lower gigahertz region, and a final frequency multiplier.

This work is devoted to an analysis of harmonically synchronized oscillators. Such a synchronization is based on a nonlinear interaction process of synchronizing and synchronized signals in the active device. Hence, a linearized theory as that of Kurokawa [1] for noise in fundamentally synchronized oscillators cannot be applied here. The nonlinearity must fully be accounted for instead.

Our theory is a phenomenological one. The shape of the nonlinearity is arbitrary; it may be single valued or double valued as for Gunn elements, *N* shaped, or *S* shaped. The nonlinearity is assumed to be incorporated into a one-port network (representing a negative resistance device), although the theory can be modified to include a two-port network, likewise. The mathematical treatment of the problem consists of two parts. First, the RF carrier signals will be calculated by using the describing function method [2]. The nonlinearity is then replaced by a periodically driven network, which allows a linear analysis for the small sideband noise or modulation signals [3].

II. Harmonic Synchronization

It is the aim of this contribution to develop a theory which leads to a tractable description of the performance of harmonically synchronized oscillators. This oscillator model shall complete the linearized model of Kurokawa with respect to including inherently nonlinear effects as harmonic (or subharmonic) synchronization. It is based on a simple equivalent circuit, which is shown in Fig. 1. The resonance structure is approximated by a parallel *LC* circuit with load conductance G_L; *N* is the active device, and v_i is a synchronizing voltage source. The active device shall be described by a cubic (van der Pol) current–voltage characteristic, relating the normalized device current y to the normalized device voltage x via

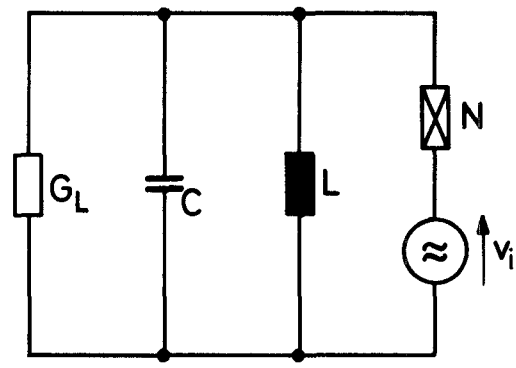

Fig. 1. Equivalent circuit of an harmonically synchronized oscillator.

$$y = -x + ax^2 + x^3 = f(x). \tag{1}$$

The normalizing quantities have been chosen according to [4]. "a" is a dimensionless parameter.

The equivalent circuit of the synchronized oscillator may in fact be as general as necessary. It may, for example, even contain nonreciprocal elements. Only two assumptions have to be made in the analysis.

1) The nonlinear characteristic is known either analytically or by numerical approximation.

2) The filtering effect of the linear part of the network is such that the voltage waveform across the active device can be found.

The oscillation amplitude can then be calculated by using the describing function method [2]. The voltage waveform being known, the current waveform is calculated by Fourier analysis using (1). Then the fundamental components of current and voltage are related by the so-called describing function n, which is the effective admittance of the nonlinear device. By setting

$$x = \hat{x}_1 \cos(\omega t + \varphi) + \hat{x}_i \cos(m\omega t) \tag{2}$$

with m as an integer, the normalized effective admittance n can be calculated. It depends on $\hat{x}_1, \hat{x}_i$ and φ for $m=2$ and $m=3$. Synchronization with higher harmonics cannot be described by a cubic nonlinearity because n turns out to be purely real in these cases. This means that the oscillation frequency cannot be tuned away from the

Manuscript received May 30, 1978. This paper was supported in part by the Deutsche Forschungsgemeinschaft.

The authors are with the Institut für Hochfrequenztechnik, Technische Universität, Postfach 3329, D-3300 Braunschweig, Germany.

0018-9480/78/1200-0939$00.75 ©1978 IEEE

natural frequency of the LC circuit; synchronization is not possible. In order to treat synchronization with $m>3$, higher order terms in the characteristic (1) have to be retained.

The describing function is defined via

$$n=\frac{1}{\pi\hat{x}_1}\int_{-\pi}^{\pi} f(x)\cos(\omega t)\,d(\omega t). \tag{3}$$

Inserting (2) yields

$$n(m=2)=-1+a\hat{x}_i e^{-2j\varphi}+\tfrac{3}{4}\hat{x}_1^2+\tfrac{3}{2}\hat{x}_i^2 \tag{4a}$$

$$n(m=3)=-1+\tfrac{3}{4}\hat{x}_1^2+\tfrac{3}{2}\hat{x}_i^2+\tfrac{3}{4}\hat{x}_1\hat{x}_i e^{-3j\varphi} \tag{4b}$$

$$n(m>3)=-1+\tfrac{3}{4}\hat{x}_1^2+\tfrac{3}{2}\hat{x}_i^2. \tag{4c}$$

The oscillation condition is obtained by applying Kirchhoff's voltage law to the equivalent circuit.

$$n+g_L(1+j\kappa)=0 \tag{5}$$

with

$$\kappa=Q_L(\nu-1/\nu)\quad Q_L=\frac{\omega_0 C}{G_L}\quad \omega_0=1/\sqrt{LC}\quad \nu=\omega/\omega_0.$$

g_L is the normalized load conductance.

Solving (5) for $\hat{x}_i=0$ yields the free-running voltage amplitude $\hat{x}_1$ and $\nu=1$. In the case of a cubic nonlinearity ($a=0$), the output power is maximum for $g_L=1/2$ and $\hat{x}_1^2=2/3$. This amplitude will be used for a further normalization.

$$X_1=\frac{\hat{x}_1^2}{2/3}\quad X_i=\frac{\hat{x}_i^2}{2/3}. \tag{6}$$

In the case of a nonzero injection voltage, the oscillation condition can directly be solved for X_1.

$$X_1=1-2X_i\pm\sqrt{8aX_i/3-\kappa^2}\,,\qquad \text{for } m=2 \tag{7a}$$

$$X_1=1-\tfrac{3}{2}X_i\pm\sqrt{X_i-7X_i^2/4-\kappa^2}\,,\qquad \text{for } m=3. \tag{7b}$$

In either case the output phase is given by

$$\tan(m\varphi)=\kappa/(1-X_1-2X_i). \tag{8}$$

From (8), the group delay distortion can be derived by differentiating the phase with respect to the frequency.

III. Stability

Equations (7) and (8) are valid provided that the oscillator is locked to the injection signal. To obtain stability conditions, the circuit is tested to see if additional injected perturbation signals of a small amplitude will grow or die away with time. Unfortunately, a disadvantage of the describing function method is that it does not allow one to determine the stable synchronization range [1]. We will hence describe a new stability criterion which is based on the conservation of power. The method is based on one of the most general minimum principles of physics, the Gaussian principle of the least constraint. Although it has originally been formulated in analytical mechanics, it can be transferred to electromagnetic theory. Here the constraint Z turns out to be the first time derivative of the power P [5].

$$Z=dP/dt. \tag{9}$$

The Gaussian principle of the least constraint then reads

$$\partial Z=\partial(dP/dt)=0 \tag{10}$$

i.e., the first variation of the constraint vanishes.

Applying (10) to oscillatory systems yields information about their stability. To this end the oscillator and the locking source are surrounded by a boundary surface. This leads to a closed system whose state is characterized by a complex power balance equation. Writing the total power as

$$P=P_a+jP_r-\mathrm{Re}(P_i)-j\,\mathrm{Im}(P_i) \tag{11}$$

with P_a the active, P_r the reactive, and P_i the injected power, the principle of conservation of energy $P=0$ yields the already-known voltage amplitude and phase.

The total power in (11) depends on both the voltage amplitude and the oscillation frequency. In order to evaluate (10), we regard a small perturbation of the operating point. The new state is characterized by a complex frequency [1] $\omega=\omega_r-j\alpha$. Equation (10) then yields two relations with $\delta\omega_r$, $\delta\alpha$, and $\delta\hat{x}_1$ as variables, which are combined in order to eliminate $\delta\omega_r$. A stability criterion can be gained from this relation if one takes into account that an increase in x_1 must cause an increase in the damping term $e^{\alpha t}$. Thus the stable synchronization range can be determined as a function of P_i or x_i. For further details, the reader is referred to [6].

In the case of harmonic synchronization, the stability condition turns out to be rather lengthy. It can be simplified considerably, however, if one follows the guideline given in [7]. It has been shown there for the case of fundamental synchronization, that the stable synchronization range is a frequency band whose upper and lower bound is characterized by an infinite slope in the amplitude curves $X_1(\nu)$. Such an equivalence can likewise be established between the amplitude curves for harmonic synchronization and the stability condition based on the Gaussian principle of the least constraint. The stable synchronization range $\Delta\nu$ can then be calculated from (7).

$$\Delta\nu\simeq 2\sqrt{a}\;\hat{x}_i/Q_L,\qquad \text{for } m=2 \tag{12a}$$

$$\Delta\nu\simeq\frac{3}{2}\hat{x}_i/Q_L\sqrt{1-21\hat{x}_i^2/8}\,,\qquad \text{for } m=3. \tag{12b}$$

The factor $\hat{x}_i/Q_L$ corresponds to $\sqrt{P_i}/Q_L$, which has been derived in [1] for fundamentally synchronized oscillators with small injection power.

IV. Noise Performance

In order to investigate the noise performance of harmonically synchronized oscillators, sideband vectors of small magnitude and stochastic phase are introduced as perturbations of the carrier signals. The calculation closely follows the pattern first introduced into oscillator

theory by Hines [8]. The noise mechanism in the active device is taken into account by equivalent sideband noise voltage sources. These sources have to be thought of as being in series to the locking voltage source v_i in Fig. 1. We are thus capable of describing both intrinsic and injected noise in a similar way. While the latter is superposed on the locking signal (the sidebands are hence located at $m\omega \pm \Omega$ with Ω being the distance to carrier frequency), the former exists not only close to the fundamental frequency but also close to its harmonics; the intrinsic noise vectors must be assumed to be located at $i\omega \pm \Omega$ with $i = 1,2,3, \cdots$. This is valid as the spectrum of the intrinsic noise is white.

The parametric mixing process between the various noise vectors is described by linear matrix algebra. The size of the computations is considerably reduced in the case, that the equivalent circuit of Fig. 1 is analyzed in conjunction with a cubic nonlinearity. Superposing small perturbation currents Δy and voltages Δx on the carrier signals y and x means for (1) that

$$y + \Delta y = f(x + \Delta x), \qquad \Delta y \ll y \qquad \Delta x \ll x. \tag{13}$$

Equation (13) can be linearized with respect to the noise signals.

$$y = f'(x)\Delta x, \qquad f'(x) = df/dx = -1 + 2ax + 3x^2 \tag{14}$$

where $f'(x)$ is a periodic function of time and may hence be expanded into a Fourier series. In the case of the cubic nonlinearity, the Fourier series is finite with coefficients $g_k = 0$ for $k \geqslant 2m+1$. The highest pair of sidebands, which must be taken into account, is hence located at $2m\omega \pm \Omega$.

The scheme for analyzing the equivalent circuit of Fig. 1 for the noise signals is the following. At the nonlinear element, the noise currents at frequencies $i\omega \pm \Omega$ with $i = 1$ to $2m$ are related to the noise voltages by a matrix equation with g_k being the elements of the conversion matrix. These equations are completed by Kirchhoff's voltage law. The upper and lower sideband voltages at the fundamental frequency Δx_u and Δx_l can then be calculated by superposing the contributions from the various sideband pairs of noise voltage sources. Finally, one has to average over the stochastic phases of the noise sources. The fundamental relations of this procedure are given in the Appendix.

The AM noise spectrum is calculated from

$$\phi_{AM} \simeq \langle \mathrm{Re}(\Delta x_u + \Delta x_l)^2 \rangle \tag{15a}$$

and the PM noise spectrum from

$$\phi_{PM} \simeq \langle \mathrm{Im}(\Delta x_u + \Delta x_l)^2 \rangle. \tag{15b}$$

The brackets denote an average over the independent phase angles of the noise voltage sources.

AM to PM and PM to AM conversion can be calculated, when the injected noise is assumed to be either purely AM or purely PM. In the former case, the pair of injected sideband sources is given by

$$\Delta x_{iu} \simeq e^{-j\gamma} \quad \Delta x_{il} \simeq e^{j\gamma}, \qquad \mathrm{AM} \tag{16}$$

and in the latter by

$$\Delta x_{iu} \simeq e^{-j\gamma} \quad \Delta x_{il} \simeq -e^{j\gamma}, \qquad \mathrm{PM}. \tag{17}$$

γ is the common stochastic phase.

Simple expressions for the noise spectra can be given for some special cases. If one takes only the intrinsic noise close to the fundamental frequency into account, the output noise is given by

$$\phi_{AM} \simeq \left(\frac{g_L}{g_0 + g_L + g_2} \right)^2, \qquad \phi_{PM} \simeq \left(\frac{g_L}{g_0 + g_L - g_2} \right)^2, \qquad \nu = 1 \qquad \Omega \to 0. \tag{18}$$

The second expression shows the stabilizing effect of the synchronizing signal on the PM noise. For $\hat{x}_i = 0$, the denominator vanishes, because 1) g_0 is 0 [4] and 2) n is $g_0 - g_2$, as can be proven by integrating (3) by parts. The denominator then equals the left-hand side of (5). This gives rise to a sharp PM noise peak, which is considerably damped even for small injected signals. The AM noise, on the other hand, is only weakly influenced by the injected signal. Furthermore, injected AM noise leads to

$$\phi_{AM} \simeq \left[\frac{(g_1 + g_3)(g_2 - g_0 - g_L)}{(g_0 + g_L)^2 - g_2^2} \right]^2, \qquad \text{for } m = 2 \tag{19a}$$

$$\phi_{AM} \simeq \left[\frac{(g_2 + g_4)(g_2 - g_0 - g_L)}{(g_0 + g_L)^2 - g_2^2} \right]^2, \qquad \text{for } m = 3 \tag{19b}$$

and injected PM noise to

$$\phi_{PM} \simeq \left[\frac{(g_1 - g_3)(g_2 + g_0 + g_L)}{(g_0 + g_L)^2 - g_2^2} \right]^2, \qquad \text{for } m = 2 \tag{20a}$$

$$\phi_{PM} \simeq \left[\frac{(g_2 - g_4)(g_2 + g_0 + g_L)}{(g_0 + g_L)^2 - g_2^2} \right]^2, \qquad \text{for } m = 3. \tag{20b}$$

Equations (19) and (20) are valid for $\nu = 1$ and $\Omega \to 0$. ν is the normalized oscillation frequency.

V. Results

Some advantageous features of frequency division by harmonic synchronization are well known. Such a divider behaves as a power limiter and shows power gain. Furthermore, the magnitude of the stable locking range is almost as large as that of a fundamentally synchronized oscillator in the case of $m = 2$. For $m = 3$, half of this value can be obtained. Comparing with fundamental synchronization one can state, as a rule of thumb, that 10-dB more locking power is needed in order to attain equal locking ranges.

A characteristic feature of harmonic synchronization is that the locking range reaches a maximum versus the injection power. This is due to the conversion efficiency, which depends on the injected signal. A large drive of the nonlinear device reduces that portion of the injected signal, which is downconverted to the fundamental.

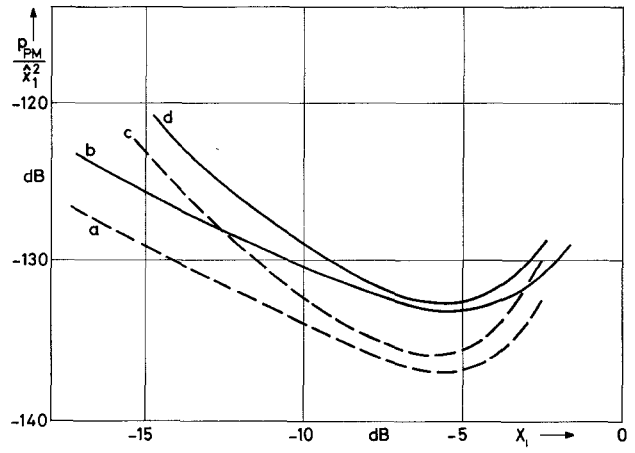

Fig. 2. Intrinsic PM sideband noise power versus the injection level for different noise contributions. $m=3$, $Q_L=10$, $g_L=0.5$, $\Omega/\omega=10^{-4}$, and $a=0$. a is for noise at ω with $\nu=1$; b is for noise at $\omega, i\omega$ with $\nu=1$; c is for noise at ω with $\nu=1.01$; d is for noise at $\omega, i\omega$ with $\nu=1.01$. $i=1$ to $2m$.

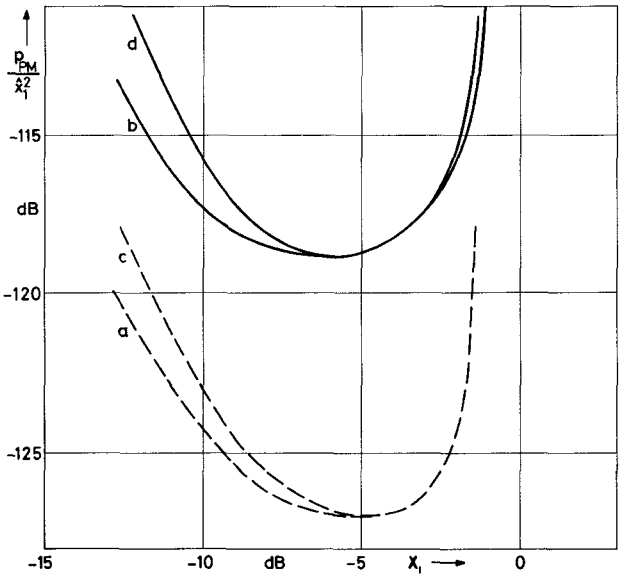

Fig. 3. Intrinsic PM sideband noise power versus the injection level for different noise contributions. $m=2$, $Q_L=10$, $g_L=0.5$, $\Omega/\omega=10^{-4}$, and $a=0.1$. a is for noise at ω with $\nu=1$: b is for noise at $\omega, i\omega$ with $\nu=1$; c is for noise at ω with $\nu=1.005$; d is for noise at $\omega, i\omega$ with $\nu=1.005$. $i=1$ to $2m$.

Hence the effective synchronizing signal decreases as does the locking range. In the case of $X_i \to 1$, the approximate formula (12a) is no longer valid. That is why (12a) shows no maximum for $\Delta\nu$ versus $\hat{x}_i$.

The maximum locking range has been computed to amount to 13 percent for $m=2$ ($a=1$), 1-dB power gain, and -1-dB output power compression, and to 4 percent for $m=3$ ($a=0$), 6-dB power gain and 0-dB output power compression. The loaded Q factor Q_L had been set to $Q_L=10$. One can nevertheless state that a gain of 10 dB should be possible. In this case, the locking range amounts to 6 percent for $m=2$ ($a=1$) and to 3 percent for $m=3$ ($a=0$), ($Q_L=10$).

The phase shift across the locking band behaves similarly as for fundamental synchronization (see (8)).

$$\tan(m\varphi) = K\kappa. \tag{21}$$

K is a function of the injection signal x_i. The group delay is smaller than for fundamental synchronization by a factor of $1/m$. The maximum shift at the borders of the locking band is $\pi/(2m)$.

The dependence of the intrinsic noise on the injected power will be discussed next. As for fundamental synchronization, the PM noise is drastically reduced, if a stable harmonic signal is injected. This is shown for $m=3$ in Fig. 2. The normalized PM sideband noise power p_{PM} has been drawn versus X_i, which is proportional to the injected power. Here and in the following the spectral density of the intrinsic noise sources has been set to $1/3 \cdot 10^{-14}$. Increasing X_i yields decreasing PM noise, until a minimum has been reached at a relatively large X_i. If X_i is increased beyond this point, the PM noise becomes worse. The explanation is the same as for the existence of a maximum of the locking range; the stabilizing effect of the injection signal depends on the conversion efficiency and hence on the drive of the nonlinear element.

It can be seen further from Fig. 2 that the noise components close to the harmonics contribute about as much to the PM noise as do the fundamental components alone. (In cases b and d, noise sources at ω and $i\omega$ with $i=2$ to $i=2m$ have been taken into account.) This effect is even more pronounced for $m=2$ as shown in Fig. 3. The normalized AM noise power p_{AM} has been drawn versus X_i in Fig. 4. Its shape is similar to that of $p_{PM}(X_i)$.

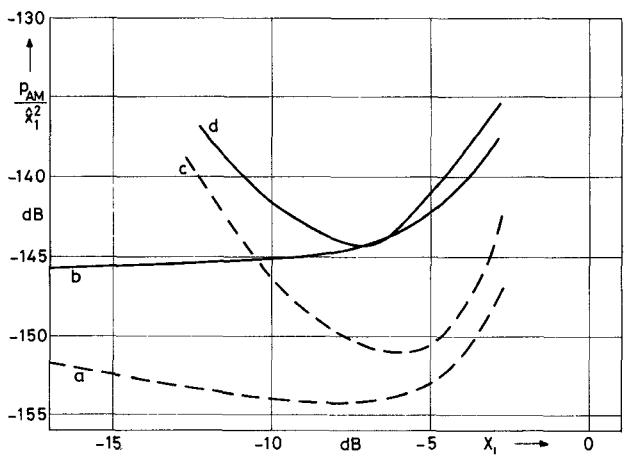

Fig. 4. Intrinsic AM sideband noise power versus the injection level for different noise contributions. $m=3$, $Q_L=10$, $g_L=0.5$, $\Omega/\omega=10^{-4}$, and $a=0$. a is for noise at ω with $\nu=1$; b is for noise at $\omega, i\omega$ with $\nu=1$; c is for noise at ω with $\nu=1.01$; d is for noise at $\omega, i\omega$ with $\nu=1.01$. $i=1$ to $2m$.

The output PM noise due to the PM noise of the injection signal is shown versus X_i in Figs. 5 and 6. (The spectral densities of the injected noises have been chosen so that the injected AM noise power[1] is -160 dB below the carrier and the injected PM noise power -128 dB.

[1]In a 1-Hz bandwidth.

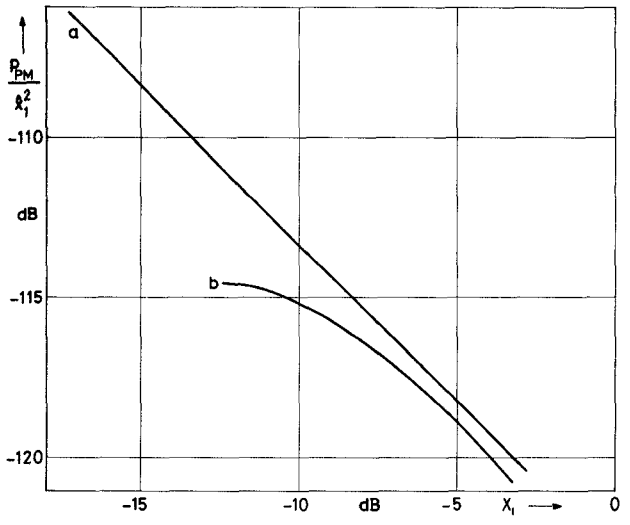

Fig. 5. PM noise power due to a PM injection signal versus the injection level. $m=3$, $Q_L=10$, $g_L=0.5$, $\Omega/\omega=10^{-4}$, and $a=0$. *a*: $\nu=1$. *b*: $\nu=1.01$.

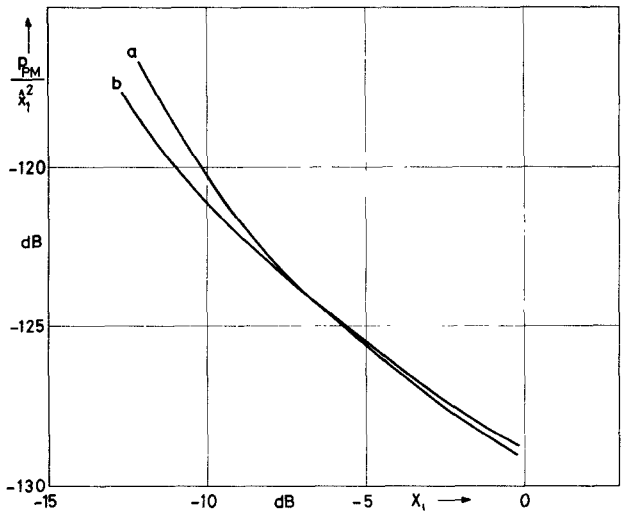

Fig. 6. PM noise power due to a PM injection signal versus the injection level. $m=2$, $Q_L=10$, $g_L=0.5$, $\Omega/\omega=10^{-4}$, and $a=0.1$ *a*: $\nu=1$. *b*: $\nu=1.005$.

This relationship is completely different from the corresponding one for fundamental synchronization, where the PM noise at the output does not depend on the injection power [9]. For harmonic synchronization, however, the PM noise monotonically decreases versus X_i. Again the explanation for this effect lies in the conversion efficiency which decreases versus X_i. Hence the PM noise which is downconverted from around $m\omega$ to ω must decrease, too. Combining the results of Figs. 2 and 5 one must suppose that the total PM noise at the output should have a minimum versus X_i. This effect could indeed be observed in practice.

An unexpected result was that the PM noise is less for $\nu \neq 1$ than for $\nu=1$, i.e., it shows a maximum in the middle of the stable locking range (see case b in Figs. 5 and 6). This is due to a very strong PM to AM conversion, which occurs for $\nu \neq 1$ at locking powers less than -10 dB. Such

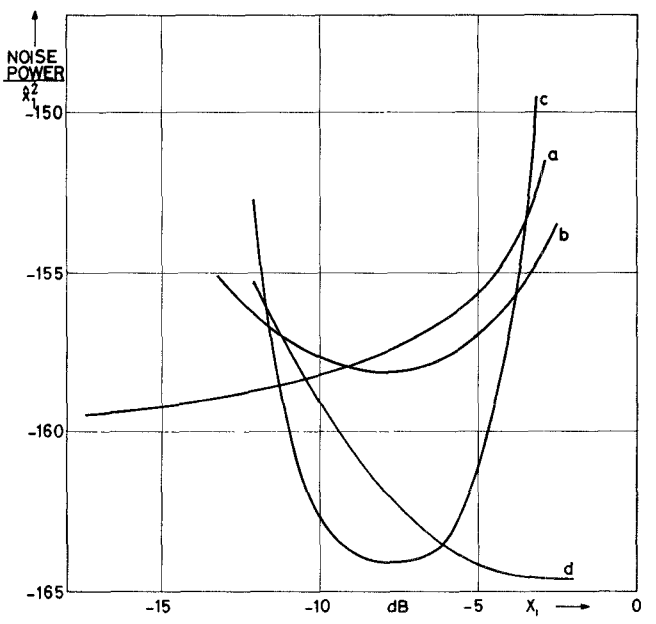

Fig. 7. AM noise power due to an AM injection signal (curves *a*, *b*), AM to PM conversion (curve *c*), and PM to AM conversion (curve *d*) versus the injection level. $m=3$, $Q_L=10$, $g_L=0.5$, $\Omega/\omega=10^{-4}$, and $a=0$. *a*: $\nu=1$ and *b*: $\nu=1.01$ (p_{AM}(AM)). *c*: $\nu=1.01$ (p_{PM}(AM)). *d*: $\nu=1.01$ (p_{AM}(PM)).

an enhancement in AM noise may impair the overall performance of the divider in practice. It has been shown for $m=3$ in Fig. 7, curve *d*. Also shown are the AM noise due to AM injection and the AM to PM conversion. Both terms increase very strongly when X_i tends to -2.5 dB. For injected powers, which exceed this margin, the oscillator cannot be synchronized any longer.

VI. Conclusions

A nonlinear model, which is capable of calculating noise and transfer properties of harmonically synchronized oscillators, has been developed. For the case where the active device is described by a van der Pol type nonlinear characteristic, analytical expressions can be derived for many of the interesting quantities. The model has been applied to both a frequency divider by a factor of 2 and a divider by a factor 3. The results show that harmonically synchronized oscillators differ in many aspects of their performance from fundamentally synchronized oscillators. This model is hoped to yield a useful tool for designing harmonic frequency divider circuits.

VII. Appendix

The coefficients of the conversion matrix are calculated from

$$g_k = \frac{1}{2\pi}\int_{-\pi}^{\pi} f'(x)e^{-jk\omega t}\,d(\omega t).$$

One obtains:

$$g_0 = -1 + \frac{3}{2}(\hat{x}_1^2 + \hat{x}_i^2)$$

$$g_1 = \left(a\hat{x}_1 + \frac{3}{2}\hat{x}_1\hat{x}_i\right)\cos\varphi + j\left(a\hat{x}_1 - \frac{3}{2}\hat{x}_1\hat{x}_i\right)\sin\varphi$$

$$g_2 = a\hat{x}_i + \frac{3}{4}\hat{x}_1^2(\cos 2\varphi + j \sin 2\varphi)$$

$$g_3 = \frac{3}{2}\hat{x}_1\hat{x}_i(\cos\varphi + j\sin\varphi) \quad g_4 = \frac{3}{4}\hat{x}_i^2 \quad g_5 = g_6 = 0, \qquad \text{for } m=2$$

and

$$g_0 = -1 + \frac{3}{2}(\hat{x}_1^2 + \hat{x}_i^2)$$

$$g_1 = a\hat{x}_1(\cos\varphi + j\sin\varphi)$$

$$g_2 = \frac{3}{4}\hat{x}_1^2(\cos 2\varphi + j\sin 2\varphi) + \frac{3}{2}\hat{x}_1\hat{x}_i(\cos\varphi - j\sin\varphi)$$

$$g_3 = a\hat{x}_i$$

$$g_4 = \frac{3}{2}\hat{x}_1\hat{x}_i(\cos\varphi + j\sin\varphi)$$

$$g_5 = 0 \quad g_6 = \frac{3}{4}\hat{x}_i^2, \qquad \text{for } m=3.$$

The matrix equation, which relates the upper and lower sideband voltages across the nonlinear device Δx_{ui} and Δx_{1i} at frequencies $i\omega \pm \Omega$ with $i=1$ to $i=2m$ to the currents Δy_{ui} and Δy_{1i}, reads

$$\begin{vmatrix} \Delta y_b \\ \Delta y_{l1} \\ \Delta y_{u1}^* \\ \Delta y_{l2} \\ \Delta y_{u2}^* \\ \Delta y_{l3} \\ \Delta y_{u3}^* \\ \Delta y_{l4} \\ \Delta y_{u4}^* \\ \Delta y_{l5} \\ \Delta y_{u5}^* \\ \Delta y_{l6} \\ \Delta y_{u6}^* \end{vmatrix} = \begin{vmatrix} g_0 & g_1^* & g_1 & g_2^* & g_2 & g_3^* & g_3 & g_4^* & g_4 & g_5^* & g_5 & g_6^* & g_6 \\ g_1 & g_0 & g_2 & g_1^* & g_3 & g_2^* & g_4 & g_3^* & g_5 & g_4^* & g_6 & g_5^* & 0 \\ g_1^* & g_2^* & g_0 & g_3^* & g_1 & g_4^* & g_2 & g_5^* & g_3 & g_6^* & g_4 & 0 & g_5 \\ g_2 & g_1 & g_3 & g_0 & g_4 & g_1^* & g_5 & g_2^* & g_6 & g_3^* & 0 & g_4^* & 0 \\ g_2^* & g_3^* & g_1^* & g_4^* & g_0 & g_5^* & g_1 & g_6^* & g_2 & 0 & g_3 & 0 & g_4 \\ g_3 & g_2 & g_4 & g_1 & g_5 & g_0 & g_6 & g_1^* & 0 & g_2^* & 0 & g_3^* & 0 \\ g_3^* & g_4^* & g_2^* & g_5^* & g_1^* & g_6^* & g_0 & 0 & g_1 & 0 & g_2 & 0 & g_3 \\ g_4 & g_3 & g_5 & g_2 & g_6 & g_1 & 0 & g_0 & 0 & g_1^* & 0 & g_2^* & 0 \\ g_4^* & g_5^* & g_3^* & g_6^* & g_2^* & 0 & g_1^* & 0 & g_0 & 0 & g_1 & 0 & g_2 \\ g_5 & g_4 & g_6 & g_3 & 0 & g_2 & 0 & g_1 & 0 & g_0 & 0 & g_1^* & 0 \\ g_5^* & g_6^* & g_4^* & 0 & g_3^* & 0 & g_2^* & 0 & g_1^* & 0 & g_0 & 0 & g_1 \\ g_6 & g_5 & 0 & g_4 & 0 & g_3 & 0 & g_2 & 0 & g_1 & 0 & g_0 & 0 \\ g_6^* & 0 & g_5^* & 0 & g_4^* & 0 & g_3^* & 0 & g_2^* & 0 & g_1^* & 0 & g_0 \end{vmatrix} \begin{vmatrix} \Delta x_b^* \\ \Delta x_{l1} \\ \Delta x_{u1}^* \\ \Delta x_{l2} \\ \Delta x_{u2}^* \\ \Delta x_{l3} \\ \Delta x_{u3}^* \\ \Delta x_{l4} \\ \Delta x_{u4}^* \\ \Delta x_{l5} \\ \Delta x_{u5}^* \\ \Delta x_{l6} \\ \Delta x_{u6}^* \end{vmatrix}.$$

Δy_b and Δx_b are sideband vectors at frequency Ω denoting noise in the bias circuit.

In writing down Kirchhoff's voltage law for the phasors at the various sideband frequencies, one has to take into account that the parallel circuit presents a finite admittance only at frequencies $\omega \pm \Omega$.

References

[1] K. Kurokawa, "Injection locking of microwave solid-state oscillators," *Proc. IEEE*, vol. 61, pp. 1386–1410, 1973.

[2] L. Gustafsson, G. H. B. Hansson, and K. I. Lundstroem, "On the use of describing functions in the study of nonlinear active microwave circuits," *IEEE Trans. Microwave Theory Tech.*, vol. MTT-20, pp. 402–409, June 1972.

[3] P. Penfield, Jr., "Circuit theory of periodically driven nonlinear systems," *Proc. IEEE*, vol. 54, pp. 266–280, 1966.

[4] M. E. Hines, "Negative-resistance diode power amplification," *IEEE Trans. Electron Devices*, vol. ED-17, pp. 1–8, Jan. 1970.

[5] H. Teichmann, "Das Gauss'sche Prinzip des kleinsten Zwanges und die Möglichkeiten seiner Anwendung auf elektrotechnische Probleme," *Arch. Elektrotech.*, vol. 44, pp. 275–278, 1959.

[6] R. Knoechel, "Analysis of stability and performance of oscillators using the Gaussian principle of the least constraint," to be presented at the 6th Microwave Colloquium, Budapest, 1978.

[7] L. Gustafsson, K. I. Lundstroem, and G. H. B. Hansson, "Maximum phase-locking bandwidth obtainable by injection locking," *IEEE Trans. Microwave Theory Tech.*, vol. MTT-21, pp. 353–355, May 1973.

[8] M. E. Hines, "Large-signal noise, frequency conversion, and parametric instabilities in IMPATT diode networks," *Proc. IEEE*, vol. 60, pp. 1534–1548, 1972.

[9] J. J. Goedbloed and M. T. Vlaardingerbroek, "Theory of noise and transfer properties of IMPATT diode amplifiers," *IEEE Trans. Microwave Theory Tech.*, vol. MTT-25, pp. 324–332, Apr. 1977.